

Kinetic and Thermodynamic Acidity of Hydrido Transition-Metal Complexes. 6. Interstitial Hydrides

Rolf T. Weberg and Jack R. Norton*

Contribution from the Department of Chemistry, Colorado State University, Fort Collins, Colorado 80523. Received April 28, 1989

Abstract: The proton-transfer behavior of interstitial hydrogens is a straightforward extension of the behavior observed previously for other types of hydride ligands. The pK_a in CH_3CN for removal of the first interstitial hydrogen from $[H_3Rh_{13}(CO)_{24}]^{2-}$ is 11.0, while the pK_a for removal of another interstitial hydrogen from $[H_2Rh_{13}(CO)_{24}]^{3-}$ is 16.5. The intrinsic barrier (the barrier to be expected if the reaction were thermoneutral) for proton transfer from $[H_3Rh_{13}(CO)_{24}]^{2-}$ to aniline is 21.3 kcal/mol, about twice the value found for terminal hydride ligands. Deprotonation of $[H_3Rh_{13}(CO)_{24}]^{2-}$ by $PhNH_2$ is thus seven orders of magnitude slower than deprotonation of $H_2Fe(CO)_4$, a mononuclear hydride complex with a pK_a comparable to that of $[H_3Rh_{13}(CO)_{24}]^{2-}$. Removal of these interstitial hydrogens by base is thus very slow despite their low pK_a values.

Previous work^{1a,2} has implied that bridging hydride ligands that leave symmetrically delocalized polynuclear anions upon deprotonation are stronger acids thermodynamically than their terminal, mononuclear, counterparts. For example, the edge-bridging hydrides in $H_4Ru_4(CO)_{12-x}(P(OMe)_3)_x$ have CH_3CN pK_a values (12.4 for $x = 1$ and 15.4 for $x = 2$)^{1c} substantially smaller than that of the terminal hydride ligands in the mononuclear $H_2Ru(CO)_4$ (18.7).^{1c} However, the same delocalization that stabilizes such symmetrically delocalized polynuclear anions obliges them to undergo relatively extensive structural and electronic reorganization in the transition state when they are protonated. One thus expects such protonation reactions, and their reverse, the deprotonation of bridging hydrides to delocalized polynuclear anions, to be even more sluggish than other proton-transfer reactions involving transition metals. Thus the bridging hydride ligands in $H_4Ru_4(CO)_{11}(P(OMe)_3)_3$ are, despite their lower pK_a , deprotonated 10^4 more slowly by $PhNH_2$ (CH_3CN , 25 °C) than the terminal hydrides in $H_2Ru(CO)_4$.^{1d,e,2,3}

This reasoning can be straightforwardly extended to "interstitial" hydride ligands such as the ones in $[HCo_6(CO)_{15}]^{-,4}$, $[HOs_{10}C(CO)_{24}]^-$ and $HOs_{10}C(CO)_{24}AuPPh_3$,⁵ $[HRu_6(CO)_{18}]^{-,6}$, $[Ni_{12}(CO)_{21}H]^{2-}$ and $[Ni_{12}(CO)_{21}H_2]^{2-,7}$ and $[Rh_{13}(CO)_{24}H_{5-n}]^{n-}$ ($n = 2, 3, 4$)⁸⁻¹⁰ (Figures 1 and 2) and $[HRh_{14}(CO)_{25}]^{-,11}$. These

hydride ligands occupy the holes within a framework of transition-metal atoms—frequently migrating rapidly among several such holes⁹—and have been advanced as models for hydrogen diffusion within bulk metals.¹⁰ One would expect such interstitial hydride ligands to be even more acidic, thermodynamically, than μ_2 hydride bridges since the negative charge resulting from the deprotonation of the interstitial hydrides can be delocalized over a larger number of metal centers. One would also expect interstitial hydride ligands to be deprotonated even more slowly than μ_2 hydride bridges (to be even less acidic, kinetically) because the structural and electronic reorganization that must occur in the transition state for the deprotonation of the former is even more extensive.

The extent of the required structural reorganization is illustrated by bond length data. Insertion of a proton into an interstitial cavity increases the surrounding metal-metal distances. For example, in the $[Rh_{13}(CO)_{24}H_{5-n}]^{n-}$ ($n = 2, 3, 4$) series the mean Rh-Rh distance increases from approximately 2.77 Å around unoccupied cavities to approximately 2.84 Å around ones occupied by hydride ligands.^{8c}

In addition to the slow rates predicted for these proton-transfer reactions, there are other reasons for interest in the interconversion of interstitial hydride ligands and external protons. In a series of papers published between 1968 and 1974 Mays and co-workers¹² suggested that high kinetic isotope effects were associated with the formation of interstitial hydrides when protons tunneled into the interstices of polynuclear anions. (It has subsequently become clear^{12b,13} that such isotope effects are common when polynuclear carbonyls are protonated, regardless of the structure of the resulting polynuclear hydride.) Furthermore, the corresponding surface process, the formation of interstitial hydrogen by reduction of external protons, is common at electrodes. Russian workers have suggested that hydrogen atoms are directly introduced inside the metal lattice of hydrogen electrodes during electrolysis (eq 1),¹⁴ although most workers now believe that adsorbed hydrogen atoms are produced as intermediates (eqs 2 and 3), at least on iron and nickel electrodes.^{15,16} The surface hydrogen atoms are

(1) (a) Jordan, R. F.; Norton, J. R. *J. Am. Chem. Soc.* **1982**, *104*, 1255. (b) Jordan, R. F.; Norton, J. R. *ACS Symp. Ser.* **1982**, *198*, 403. (c) Moore, E. J.; Sullivan, J. M.; Norton, J. R. *J. Am. Chem. Soc.* **1986**, *108*, 2257. (d) Edidin, R. T.; Sullivan, J. M.; Norton, J. R. *J. Am. Chem. Soc.* **1987**, *109*, 3945. (e) Kristjānsdóttir, S. S.; Moody, A. E.; Weberg, R. T.; Norton, J. R. *Organometallics* **1988**, *7*, 1988.

(2) Walker, H. W.; Pearson, R. G.; Ford, P. C. *J. Am. Chem. Soc.* **1983**, *105*, 1179.

(3) Interestingly, a contrasting result has been reported by Walker, Pearson, and Ford: MeO^- deprotonates the bridging hydride in $H_4Os_4(CO)_{12}$ (pK_a 12.0 in MeOH) 10^2 faster than it deprotonates the terminal hydrides in $H_2Os(CO)_4$ (pK_a 15.2 in MeOH).²

(4) (a) Hart, D. W.; Teller, R. G.; Chiau-Yu, W.; Bau, R.; Longoni, G.; Campanella, S.; Chini, P.; Koetzle, T. F. *Angew. Chem., Int. Ed. Engl.* **1979**, *18*, 80. (b) Hart, D. W.; Teller, R. G.; Chiau-Yu, W.; Bau, R.; Longoni, G.; Campanella, S.; Chini, P.; Koetzle, T. F. *J. Am. Chem. Soc.* **1981**, *103*, 1458. (c) Stanghellini, P. L.; Longoni, G. *J. Chem. Soc., Dalton Trans.* **1987**, 685.

(5) Jackson, P. F.; Johnson, B. F. G.; Lewis, J.; McPartlin, M.; Nelson, W. J. *J. Chem. Soc., Chem. Commun.* **1982**, 49.

(6) (a) Eady, C. R.; Johnson, B. F. G.; Lewis, J.; Malatesta, M. C.; Machin, P.; McPartlin, M. *J. Chem. Soc., Chem. Commun.* **1976**, 945. (b) Jackson, P. F.; Johnson, B. F. G.; Lewis, J.; Raithby, P. R.; McPartlin, M.; Nelson, W. J. H.; Rouse, K. D.; Allibon, J.; Mason, S. A. *J. Chem. Soc., Chem. Commun.* **1980**, 295.

(7) Broach, R. W.; Dahl, L. F.; Longoni, G.; Chini, P.; Schultz, A. J.; Williams, J. M. *Adv. Chem. Ser.* **1978**, *167*, 93.

(8) (a) Albano, V. G.; Ceriotti, A.; Chini, P.; Ciani, G.; Martinengo, S.; Anker, W. M. *J. Chem. Soc., Chem. Commun.* **1975**, 859. (b) Albano, V. G.; Ciani, G.; Martinengo, S.; Sironi, A. *J. Chem. Soc., Dalton Trans.* **1979**, 978. (c) Ciani, G.; Sironi, A.; Martinengo, S. *J. Chem. Soc., Dalton Trans.* **1981**, 519.

(9) (a) Martinengo, S.; Heaton, B. T.; Goodfellow, R. J.; Chini, P. *J. Chem. Soc., Chem. Commun.* **1977**, 39. (b) Allevi, C.; Heaton, B. T.; Seregni, C.; Strona, L.; Goodfellow, R. J.; Chini, P.; Martinengo, S. *J. Chem. Soc., Dalton Trans.* **1986**, 1375.

(10) (a) Chini, P. *Gazz. Chim. Ital.* **1979**, *109*, 225. (b) Chini, P.; Longoni, G.; Martinengo, S.; Ceriotti, A. *Adv. Chem. Ser.* **1978**, *167*, 1. (c) Chini, P.; Longoni, G.; Martinengo, S. *Chim. Ind. (Milan)* **1978**, *60*, 989-97. (d) Chini, P. *J. Organomet. Chem.* **1980**, *200*, 37-61.

(11) Ciani, G.; Sironi, A.; Martinengo, S. *J. Organomet. Chem.* **1980**, *192*, C42.

(12) (a) Mays, M. J.; Simpson, R. N. *F. J. Chem. Soc. A* **1968**, 1444. (b) Knight, J.; Mays, M. J. *J. Chem. Soc. A* **1970**, 711. (c) Cooke, C. G.; Mays, M. J. *J. Organomet. Chem.* **1974**, *74*, 449.

(13) Pribich, D. C.; Rosenberg, E. *Organometallics* **1988**, *7*, 1741.

(14) (a) Bagotskaya, I. A. *Zh. Fiz. Khim.* **1962**, *36*, 2667; *Russ. J. Phys. Chem.* **1962**, *36*, 1447. (b) Kovba, L. D. *Zh. Fiz. Khim.* **1963**, *37*, 161; *Russ. J. Phys. Chem.* **1963**, *37*, 76. (c) Frumkin, A. N. *Advances in Electrochemistry and Electrochemical Engineering*; Delahay, P., Ed.; Vol. 3; Interscience: New York, 1963; Vol. 3, p 287.

(15) (a) McBreen, J.; Genshaw, M. A. *Fundamental Aspects of Stress Corrosion Cracking*; Staehle, R. W., Ed.; NACE: Houston, TX, 1969; pp 51-63. (b) Bockris, J. O'M.; Reddy, A. K. N. *Modern Electrochemistry*; Plenum: New York, 1970; pp 1231-1253.

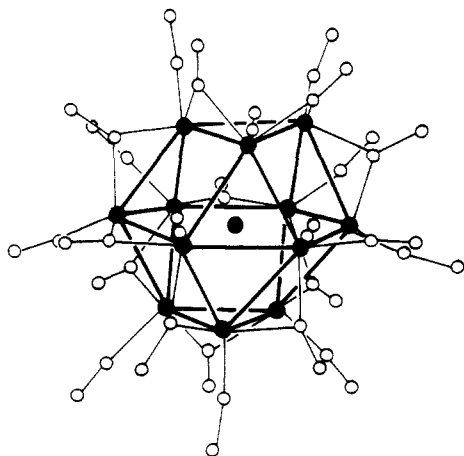


Figure 1. Structure of $[\text{Rh}_{13}(\text{CO})_{24}\text{H}_3]^{2-}$ (ref 8a) (reproduced from *Adv. Chem. Ser.* **1978**, 167, 1; copyright 1978 by the American Chemical Society).

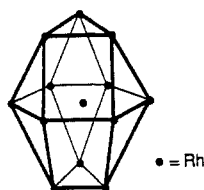


Figure 2. The hexagonal-close-packed Rh_{13} core of $[\text{Rh}_{13}(\text{CO})_{24}\text{H}_{5-n}]^{n-}$. Six pseudooctahedral holes lie inside the six square faces, and eight tetrahedral holes lie inside the eight triangular faces.

in rapid equilibrium with lattice hydrogen atoms directly beneath them, whereas diffusion of the hydrogen atoms throughout the lattice is comparatively slow. The transformation during electrolysis of a solution proton into a lattice hydrogen directly beneath the electrode surface is modeled by the insertion of a proton into a cavity of a discrete metal cluster; both types of interstitial site adjoin an edge.



The first interstitial hydride cluster we selected for the quantitative study of its acidity was $[\text{HCo}_6(\text{CO})_{15}]^-$. X-ray and neutron-diffraction studies had shown the hydrogen atom to be located at the center of the cobalt octahedron.⁴ The dianion, $[\text{Co}_6(\text{CO})_{15}]^{2-}$, was known to be easily protonated to give $[\text{HCo}_6(\text{CO})_{15}]^-$ which, in turn, was readily deprotonated upon dissolution in water, methanol, or tetrahydrofuran.^{4b} Chini and co-workers had predicted that a cluster with all of the available interstitial holes occupied by hydrogen atoms would be relatively unstable,¹⁰ which suggested that $[\text{HCo}_6(\text{CO})_{15}]^-$ would be a relatively strong acid.

Perhaps for the reasons Chini suggested, the Co_6 framework of $[\text{HCo}_6(\text{CO})_{15}]^-$ proved unstable in $\text{H}_2\text{O}/\text{THF}$ or CH_3CN solution, making quantitative studies impossible. We therefore examined the $[\text{Rh}_{13}(\text{CO})_{24}\text{H}_{5-n}]^{n-}$ series,⁸⁻¹⁰ several members of which ($n = 2, 3,$ and 4) are suitably stable in solution. As shown in Figures 1 and 2, the rhodium atoms of these clusters form hexagonal-close-packed arrays, with six pseudooctahedral holes (i.e., octahedral holes surrounded by only five rhodium atoms instead of six) and eight tetrahedral holes. Structural⁸ and ¹H NMR⁹ data imply that the hydride ligands occupy the pseudooctahedral holes and move readily between them, presumably by jumping through the tetrahedral holes. Results already in the literature suggested that $[\text{Rh}_{13}(\text{CO})_{24}\text{H}_3]^{2-}$ was a fairly strong

Table I. Carbonyl Stretching Frequencies and Absorptivities in CH_3CN

	$[\text{Rh}_{13}(\text{CO})_{24}\text{H}_3]^{2-}$	$[\text{Rh}_{13}(\text{CO})_{24}\text{H}_2]^{3-}$	$[\text{Rh}_{13}(\text{CO})_{24}\text{H}]^{4-}$
terminal ν_{CO} , cm^{-1}	2019 ^a	1992 ^b	1964 ^a
bridging CO, cm^{-1}	1840 ^a	1813 ^b	
ϵ_{2019} , $\text{M}^{-1} \text{cm}^{-1}$	32450	2798	
ϵ_{1992} , $\text{M}^{-1} \text{cm}^{-1}$	3657	35880	

^a These values agree well with those originally reported in ref 8a and 10a in THF. ^b These values agree well with those originally reported in ref 8a in the same solvent.

Table II. pK_a Values of Interstitial Rhodium Hydride Clusters (CH_3CN , 25 °C)

	$[\text{Rh}_{13}(\text{CO})_{24}\text{H}_3]^{2-}$	$[\text{Rh}_{13}(\text{CO})_{24}\text{H}_2]^{3-}$
base	<i>p</i> - $\text{CF}_3\text{C}_6\text{H}_4\text{NH}_2$	pyridine
$\text{pK}_a(\text{BH}^+)$	8.6 (1) ^{c,d}	12.33 ¹⁸
$K_f(\text{BHB}^+)$		0.6 ¹⁷
$\text{pK}_a(\text{hydride})$	11.0 (2)	16.5 (1)

acid: Chini and co-workers obtained a potentiometric titration curve similar to that of perchloric acid when they titrated $[\text{Rh}_{13}(\text{CO})_{24}\text{H}_3]^{2-}$ with dilute KOH in 3:1 dmsu/water.^{10c}

Results

Thermodynamic Acidity of $[\text{H}_n\text{Rh}_{13}(\text{CO})_{24}]^{(5-n)-}$. The series of tridecanuclear cluster anions, $[\text{H}_n\text{Rh}_{13}(\text{CO})_{24}]^{(5-n)-}$ ($n = 1-4$), has proven amenable to thermodynamic and kinetic acidity measurements in acetonitrile. The $\text{H}_2\text{Rh}_{13}^{3-}$ and $\text{H}_3\text{Rh}_{13}^{2-}$ clusters are stable indefinitely in that solvent, and the $\text{H}_1\text{Rh}_{13}^{4-}$ one is stable for a few hours. Each of the three clusters has an IR spectrum in CH_3CN (Table I) consisting of one intense terminal carbonyl stretch and a broad, lower frequency bridging carbonyl stretch. The frequencies of both bands decrease by about 27 cm^{-1} for each proton removed.

It was thus convenient to follow all deprotonation reactions by monitoring the terminal carbonyl region of the IR spectrum. Only the $\text{H}_2\text{Rh}_{13}^{3-}$ and $\text{H}_3\text{Rh}_{13}^{2-}$ clusters were stable enough in acetonitrile to permit the direct measurement of their molar absorptivities. The absorptivities of both species were determined at 2019 cm^{-1} (the absorption maximum for $\text{H}_3\text{Rh}_{13}^{2-}$) and 1992 cm^{-1} (the absorption maximum for $\text{H}_2\text{Rh}_{13}^{3-}$), so that the concentrations of both $\text{H}_2\text{Rh}_{13}^{3-}$ and $\text{H}_3\text{Rh}_{13}^{2-}$ could be determined either by measuring the absorbance at 2019 cm^{-1} (A_{2019}) and using eq 4 or by measuring the absorbance at 1992 cm^{-1} (A_{1992}) and using eq 5. (T is the total concentration of $\text{H}_2\text{Rh}_{13}^{3-}$ and $\text{H}_3\text{Rh}_{13}^{2-}$ present, and x is the mole fraction of T which is $\text{H}_3\text{Rh}_{13}^{2-}$.) The absorptivity data are presented in Table I.

$$A_{2019} = xT\epsilon_{(\text{H}_3\text{Rh}_{13}^{2-} \text{ at } 2019)} + (1-x)T\epsilon_{(\text{H}_2\text{Rh}_{13}^{3-} \text{ at } 2019)} \quad (4)$$

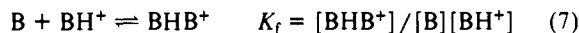
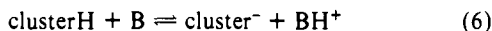
$$A_{1992} = xT\epsilon_{(\text{H}_3\text{Rh}_{13}^{2-} \text{ at } 1992)} + (1-x)T\epsilon_{(\text{H}_2\text{Rh}_{13}^{3-} \text{ at } 1992)} \quad (5)$$

The pK_a values for $\text{H}_2\text{Rh}_{13}^{3-}$ and $\text{H}_3\text{Rh}_{13}^{2-}$ in CH_3CN were determined by the methods previously employed for other hydrides.^{1a-c,e} Acetonitrile solutions of $\text{H}_2\text{Rh}_{13}^{3-}$ or $\text{H}_3\text{Rh}_{13}^{2-}$ were treated with bases that effected partial deprotonation (eq 6). When $\text{H}_3\text{Rh}_{13}^{2-}$ was being deprotonated, equilibrium concentrations of $\text{H}_2\text{Rh}_{13}^{3-}$ and $\text{H}_3\text{Rh}_{13}^{2-}$ were calculated from eqs 4 and 5; when $\text{H}_2\text{Rh}_{13}^{3-}$ was being deprotonated, the equilibrium concentration of $\text{H}_2\text{Rh}_{13}^{3-}$ was calculated from $\epsilon_{(\text{H}_2\text{Rh}_{13}^{3-} \text{ at } 1992)}$ and A_{1992} , and the equilibrium concentration of $\text{H}_1\text{Rh}_{13}^{4-}$ was obtained by subtracting $[\text{H}_2\text{Rh}_{13}^{3-}]$ from the total concentration of $\text{H}_2\text{Rh}_{13}^{3-}$ initially present. The concentration of free base ($[\text{B}]$) and the concentration of protonated base ($[\text{BH}^+]$) were calculated from the concentration of deprotonated cluster ($[\text{cluster}^-]$) and the total concentration of base originally added, after correction^{17,18} for self-association (eq 7) in the case of pyridine.

(17) The correction procedure for association between py and pyH^+ has been described in detail in ref 1c; $[\text{pyHpy}^+]$ was calculated from eq 3 therein and the known¹⁸ value of the association equilibrium constant.

(18) Coetzee, J. F.; Padmanabhan, G. R.; Cunningham, G. P. *Talanta* **1964**, 11, 93.

(16) (a) Latanision, R. M.; Kurkela, L. M. *Corrosion* **1983**, 39, 174-181 and references therein. (b) Frankel, G. S.; Latanision, R. M. *Metall. Trans. A* **1986**, 17A, 861-867.



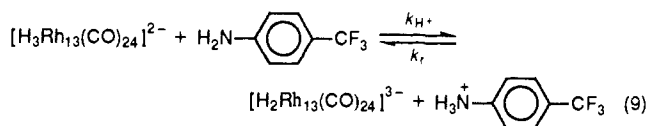
The deprotonation equilibrium constants K_{eq} were calculated from $[\text{clusterH}]$, $[\text{cluster}^-]$, $[\text{B}]$, and $[\text{BH}^+]$. The $\text{p}K_{\text{a}}$'s of the interstitial hydride clusters were then calculated from the known^{1c,d,19} $\text{p}K_{\text{a}}$ values for BH^+ according to eq 8. The results are summarized in Table II. Neither cluster $\text{p}K_{\text{a}}$ value has been corrected for the number of ionizable hydrogens.

$$\text{p}K_{\text{a}}(\text{clusterH}) = \text{p}K_{\text{a}}(\text{BH}^+) + \text{p}K_{\text{eq}} \quad (8)$$

The $\text{p}K_{\text{a}}$ value for $[\text{Rh}_{13}(\text{CO})_{24}\text{H}_2]^{3-}$ may not be as accurate (despite its higher precision) as that for $[\text{Rh}_{13}(\text{CO})_{24}\text{H}_3]^{2-}$ because of the lack of absorptivity information for $[\text{Rh}_{13}(\text{CO})_{24}\text{H}_1]^{4-}$.

Kinetic Acidity of $[\text{H}_n\text{Rh}_{13}(\text{CO})_{24}]^{(5-n)-}$. Pseudo-first-order rate constants were measured in acetonitrile solution for proton transfer from $[\text{Rh}_{13}(\text{CO})_{24}\text{H}_3]^{2-}$ to *p*-toluidine, aniline itself, and *p*-iodoaniline, each present in sufficiently large excess that the reaction went to completion. The second-order rate constants k_{H^+} for proton transfer to these bases were thereby determined.

Determination of k_{H^+} for proton transfer from $[\text{Rh}_{13}(\text{CO})_{24}\text{H}_3]^{2-}$ to *p*-CF₃C₆H₄NH₂ (eq 9) proved more complex. As *p*-CF₃C₆H₄NH₂ was more than two $\text{p}K_{\text{a}}$ units less basic than $[\text{Rh}_{13}(\text{CO})_{24}\text{H}_2]^{3-}$, the conjugate base of $[\text{Rh}_{13}(\text{CO})_{24}\text{H}_3]^{2-}$, no feasible concentration of *p*-CF₃C₆H₄NH₂ drove the equilibrium in eq 9 entirely to the right. The rate constants k_{H^+} and k_r for the $[\text{Rh}_{13}(\text{CO})_{24}\text{H}_3]^{2-}/p\text{-CF}_3\text{C}_6\text{H}_4\text{NH}_2$ system were thus extracted from approach-to-equilibrium measurements.²⁰ Values of k_{H^+} at 25 °C for aniline and all three para-substituted aniline derivatives are shown in Table III.



The data in Table III have allowed us to examine the influence of thermodynamic driving force on the rate at which interstitial hydrides are removed as protons. A plot of $\log k_{\text{H}^+}$ vs $\log K_{\text{eq}}$ ($-\text{p}K_{\text{eq}}$) is shown in Figure 3. From it can be obtained values of two parameters that have proven useful in the analysis of other types of proton-transfer reactions. For example, the slope of the plot in Figure 3, 0.46 (8), is the Brønsted coefficient α as defined in eqs 10 and 11.²¹ The intercept of the plot in Figure 3 (i.e., the value of $\log k_{\text{H}^+}$ when $-\text{p}K_{\text{eq}}$ is zero and K_{eq} is unity) gives the rate constant to be expected if the removal of a proton from an interstitial site is thermoneutral (i.e., if the reaction has a thermodynamic driving force ΔG^\ddagger equal to zero). The activation free energy corresponding to $\log k_{\text{H}^+}$ at the intercept is known²¹ as the "intrinsic barrier" ΔG_0^\ddagger . The value of ΔG_0^\ddagger calculated from the intercept of Figure 3 is 21.3 (2) kcal/mol.

$$\log k = \alpha \log K + \text{constant} \quad (10)$$

$$\alpha = \partial \Delta G^\ddagger / \partial \Delta G^\circ \quad (11)$$

The value of k_{H^+} from $[\text{Rh}_{13}(\text{CO})_{24}\text{H}_3]^{2-}$ to unsubstituted aniline was measured over a range of temperatures. The results, presented in Table IV, give an activation energy E_{a} of 15.1 (4)

Table III. Rate Constants for Deprotonation of $[\text{Rh}_{13}(\text{CO})_{24}\text{H}_3]^{2-}$ by *p*-XC₆H₄NH₂ in CH₃CN at 25 °C

X	$\text{p}K_{\text{a}}(\text{BH}^+)$	$-\text{p}K_{\text{eq}}$	k_{H^+} , M ⁻¹ s ⁻¹
CH ₃	11.1	0.2	$1.42 (8) \times 10^{-3}$
H	10.5	-0.4	$1.2 (1) \times 10^{-3}$
I	9.5	-1.4	$2.1 (2) \times 10^{-4}$
CF ₃	8.6	-2.4	$1.3 (4) \times 10^{-4}$

Table IV. Temperature Dependence of k_{H^+} for Proton Transfer from $[\text{Rh}_{13}(\text{CO})_{24}\text{H}_3]^{2-}$ to Aniline (CH₃CN, 25 °C)

T, K	k_{H^+} , M ⁻¹ s ⁻¹
298	$1.2 (1) \times 10^{-3}$
303	$1.79 (3) \times 10^{-3}$
308	$2.9 (3) \times 10^{-3}$
313	$4.1 (1) \times 10^{-3}$
318	$5.9 (1) \times 10^{-3}$

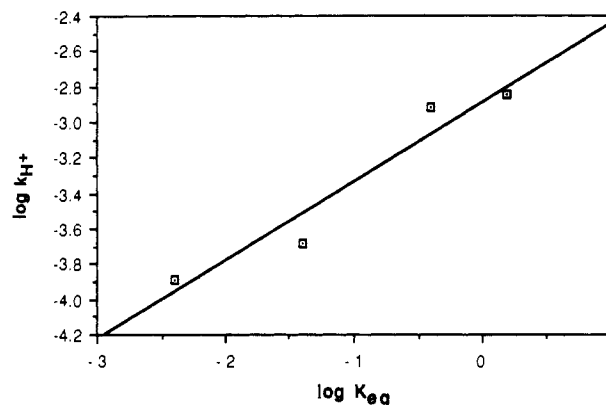


Figure 3. Brønsted plot ($\log k_{\text{H}^+}$ vs $\log K_{\text{eq}}$) for $[\text{H}_3\text{Rh}_{13}(\text{CO})_{24}]^{2-}$ deprotonation by para-substituted anilines.

kcal/mol with a preexponential factor A of 1.52×10^8 M⁻¹ s⁻¹, or an activation enthalpy ΔH^\ddagger of 14.5 (4) kcal/mol with an activation entropy ΔS^\ddagger of -23 (1) eu.

Conclusions

The proton-transfer behavior of interstitial hydrides is a straightforward extension of the behavior observed previously for other types of hydride ligands.^{1,2} Thermodynamically, the acidity of the interstitial hydrogens in $[\text{H}_3\text{Rh}_{13}(\text{CO})_{24}]^{2-}$ ($\text{p}K_{\text{a}}$ in CH₃CN = 11.0) is comparable to that of the bridging hydrides in $(\mu\text{-H})_2\text{Fe}_3(\text{CO})_9(\mu_3\text{-P-}t\text{-Bu})$ ($\text{p}K_{\text{a}}$ in CH₃CN = 11.4^{1e}). In both cases the conjugate base is a polynuclear anion with a highly delocalized negative charge.

Not surprisingly, the removal of one proton from $[\text{H}_3\text{Rh}_{13}(\text{CO})_{24}]^{2-}$ makes the remaining interstitial hydrogens less acidic; the increase in $\text{p}K_{\text{a}}$ from $[\text{H}_3\text{Rh}_{13}(\text{CO})_{24}]^{2-}$ to $[\text{H}_2\text{Rh}_{13}(\text{CO})_{24}]^{3-}$ is more than five units. Extrapolation of this pattern in the opposite direction, to more highly protonated members of the $[\text{Rh}_{13}(\text{CO})_{24}\text{H}_{5-n}]^{n-}$ series, suggests that the hypothetical $[\text{Rh}_{13}(\text{CO})_{24}\text{H}_4]^-$ should have a lower $\text{p}K_{\text{a}}$ than HCo(CO)₄ and that the hypothetical $\text{Rh}_{13}(\text{CO})_{24}\text{H}_5$ should be a fully dissociated strong acid in acetonitrile.

The difference in $\text{p}K_{\text{a}}$ between $[\text{Rh}_{13}(\text{CO})_{24}\text{H}_3]^{2-}$ and $[\text{Rh}_{13}(\text{CO})_{24}\text{H}_2]^{3-}$ in CH₃CN is virtually the same as the difference between the successive dissociation constants in H₂O of very different species, single-centered oxyacids with several ionizable protons. The inorganic oxyacid interval is known to be constant at about five $\text{p}K_{\text{a}}$ units.²² For example, the first $\text{p}K_{\text{a}}$ of H₃PO₄ in H₂O is 2.1, the second 7.2, and the third 12.0.

One of the reasons that $\text{p}K_{\text{a}}$ increases as protons are removed from any polyacid is the electrostatic repulsion between multiple negative charges, and the energy of species bearing such charges

(19) (a) Coetzee, J. F. *Prog. Phys. Org. Chem.* **1967**, *4*, 45. (b) Coetzee, J. R.; Padmanabhan, G. R. *J. Am. Chem. Soc.* **1965**, *87*, 5005.

(20) The data for deprotonation by *p*-iodoaniline, the next-weakest base, were also treated by the same approach-to-equilibrium methods. The resulting value of k_{H^+} was within experimental error of the one that had been obtained by a pseudo-first-order treatment. The large excess of *p*-IC₆H₄NH₂ used must thus (as predicted by the $\text{p}K_{\text{a}}$ values) have led to virtually complete deprotonation of the $[\text{Rh}_{13}(\text{CO})_{24}\text{H}_3]^{2-}$.

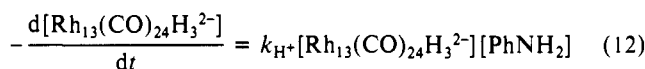
(21) Clear definitions of the Brønsted coefficient α and the intrinsic barrier ΔG_0^\ddagger , along with explanations of eqs 11, 13, and 14, have been given by: Kresge, A. J. *Chem. Soc. Rev.* **1973**, *2*, 475. The term "intrinsic barrier" was introduced by Marcus in an early account of what has become known as Marcus theory: Marcus, R. A. *J. Phys. Chem.* **1968**, *72*, 891. Calculations of intrinsic barriers for proton transfer between transition metals have just been published: Creutz, C.; Sutin, N. *J. Am. Chem. Soc.* **1988**, *110*, 2418.

(22) (a) Pauling, L.; Pauling, P. *Chemistry*; Freeman: San Francisco, 1975; p 394. (b) Greenwood, N. N.; Earnshaw, A. *Chemistry of the Elements*; Pergamon: New York, 1984; pp 52-55. (c) Freiser, H.; Fernando, Q. *Ionic Equilibria in Analytical Chemistry*; Wiley: New York, 1963; pp 80-81.

should be especially high in acetonitrile, as that solvent is known to solvate cations effectively but anions poorly.^{19a} Thus the more highly charged members of the $[\text{Rh}_{13}(\text{CO})_{24}\text{H}_{5-n}]^{n-}$ series (e.g., $[\text{Rh}_{13}(\text{CO})_{24}\text{H}]^{4-}$) are unstable in CH_3CN , and negatively charged rhodium carbonyl clusters of higher nuclearity frequently dissociate into fragments in that solvent.^{9b,10a}

The polyacids most suited for comparison of their $\text{p}K_a$ intervals with that of the $[\text{Rh}_{13}(\text{CO})_{24}\text{H}_{5-n}]^{n-}$ series should be other large polynuclear arrays with similar ability to delocalize charge. The successive dissociation constants for the ionization of the triprotonated polyoxoanions $[\text{H}_3\text{PMo}_{12}\text{O}_{40}]^{4-}$ are 4.5, 6.9, and 9.3 in H_2O ²³—a constant interval of 2.4 $\text{p}K_a$ units. The larger interval found for the $[\text{Rh}_{13}(\text{CO})_{24}\text{H}_{5-n}]^{n-}$ series may mean that the negative charges are less delocalized in the rhodium series than in the molybdenum polyoxoanion series,²⁴ or it may simply reflect the lower dielectric constant²⁵ of the CH_3CN used as a solvent for the $[\text{Rh}_{13}(\text{CO})_{24}\text{H}_{5-n}]^{n-}$ measurements.

Deprotonation of $[\text{Rh}_{13}(\text{CO})_{24}\text{H}_3]^{2-}$ by aniline and its substituted derivatives obeys second-order kinetics (eq 12) up to concentrations of 0.20 M in aniline, 0.41 M in $p\text{-IC}_6\text{H}_4\text{NH}_2$, and 0.50 M in $p\text{-CF}_3\text{C}_6\text{H}_4\text{NH}_2$. There is no evidence for any rate-determining step prior to H^+ removal.²⁶



The deprotonation of $[\text{H}_3\text{Rh}_{13}(\text{CO})_{24}]^{2-}$ is much slower than would be expected for an acid with a $\text{p}K_a$ of 11.0 in CH_3CN . The mononuclear dihydride $\text{H}_2\text{Fe}(\text{CO})_4$ has a $\text{p}K_a$ of 11.4 in CH_3CN , and thus its thermodynamic driving force for proton transfer to aniline is similar to that of $[\text{H}_3\text{Rh}_{13}(\text{CO})_{24}]^{2-}$. Yet the rate constant for proton transfer to aniline from $\text{H}_2\text{Fe}(\text{CO})_4$ is $5.4 \times 10^4 \text{ M}^{-1} \text{ s}^{-1}$ while that from $[\text{H}_3\text{Rh}_{13}(\text{CO})_{24}]^{2-}$ is $1.2 \times 10^{-3} \text{ M}^{-1} \text{ s}^{-1}$ (in CH_3CN at 25 °C)—a difference of over seven orders of magnitude. The high kinetic barrier to proton transfer ΔG^\ddagger exhibited by $[\text{H}_3\text{Rh}_{13}(\text{CO})_{24}]^{2-}$ arises from its high intrinsic barrier to thermoneutral proton transfer ΔG_0^\ddagger . (The exact relationship between ΔG^\ddagger and ΔG_0^\ddagger proposed by Marcus theory²¹ is given as eq 13.) Indeed, the value of 21.3 kcal/mol for ΔG_0^\ddagger for $[\text{H}_3\text{Rh}_{13}(\text{CO})_{24}]^{2-}$ obtained from the intercept of Figure 1 is twice that observed^{1d} for mononuclear hydride species (9–11 kcal/mol).

$$\Delta G^\ddagger = (1 + \Delta G_0^\circ / 4\Delta G_0^\ddagger) \Delta G_0^\ddagger \quad (13)$$

The fact that the Brønsted coefficient α (the slope of the plot in Figure 1) is about one-half offers additional evidence that ΔG_0^\ddagger for proton removal from $[\text{H}_3\text{Rh}_{13}(\text{CO})_{24}]^{2-}$ is large. Marcus theory²¹ gives eq 14 as the relationship between α , ΔG_0^\ddagger , and ΔG_0° , and the value of α predicted from eq 14 approaches one-half as ΔG_0^\ddagger increases. The large value of the intrinsic barrier ΔG_0^\ddagger for $[\text{H}_3\text{Rh}_{13}(\text{CO})_{24}]^{2-}$ reflects the substantial electronic and structural rearrangement which must occur when an interstitial hydrogen is removed by deprotonation.

$$\alpha = \frac{\partial \Delta G^\ddagger}{\partial \Delta G_0^\circ} = \frac{1 + \Delta G_0^\circ / 4\Delta G_0^\ddagger}{2} \quad (14)$$

We are currently using our knowledge of deprotonation rates to replace H by D in the interstitial sites in these rhodium clusters. We are also planning to measure the kinetic isotope effects $k_{\text{H}}/k_{\text{D}}$ on proton transfer in and out of such interstitial sites.

(23) Fruchart, J.-M.; Souchay, P. *Compt. Rend. C* **1968**, 266, 1571.

(24) The multiple negative charges in phosphomolybdate anions are presumably concentrated on terminal oxide ligands around their periphery.

(25) Discussions, with references, of the influence of dielectric constant on the intervals between successive acid dissociation constants can be found in: (a) Cotton, F. A.; Wilkinson, G. *Advanced Inorganic Chemistry*, 4th ed.; Wiley: New York, 1981; pp 236–241. (b) Bell, R. P. *The Proton in Chemistry*; Cornell University Press: Ithaca, NY, 1973; p 96.

(26) There is thus no evidence that any rearrangement is required before an interstitial hydride can be removed as a proton. The rate constant for such a rearrangement should become rate-limiting when sufficiently large amounts of base are present. Examples of such mechanisms are known in organic chemistry, e.g., the rate-determining dissociation of a hydrogen bond before the deprotonation of "proton sponges"; see: Stewart, R. *The Proton: Applications to Organic Chemistry*; Academic: New York, 1985; p 276.

Experimental Section

General. All manipulations were carried out under inert (N_2) atmosphere with high-vacuum, Schlenk or inert-atmosphere-box techniques. Infrared spectra were recorded on a Perkin-Elmer PE983 spectrometer with a 0.01-cm CaF_2 cell.

Acetonitrile was purified with our previously reported procedure.^{16c} Aniline, p -toluidine, and $p\text{-CF}_3\text{C}_6\text{H}_4\text{NH}_2$ were dried over and then distilled from barium oxide. $\text{CO}_2(\text{CO})_8$ was sublimed prior to use. p -Iodoaniline was first acidified in, and its protonated form precipitated from, an ether solution; after addition of base to an aqueous solution of the protonated form, it was extracted into ether in its neutral form and finally recrystallized from ether. (As p -iodoaniline is light sensitive, it and its solutions were shielded from light at all times.)

Materials. $[\text{Co}_6(\text{CO})_{15}]^{2-}$ was prepared by literature methods²⁷ and isolated as either its K_2 or $[\text{PPN}]_2$ salt. Protonation by HCl in aqueous solution by the literature method⁴ gave $[\text{HCo}_6(\text{CO})_{15}]^-$. Use of the K_2 salt resulted in a higher yield of the product although, in both cases, impurities and starting material were observed at low levels by IR. $\text{Rh}_2(\text{CO})_4(\mu\text{-Cl})_2$ ²⁸ and $\text{Rh}_4(\text{CO})_{12}$ ²⁹ were prepared by literature methods. $[\text{PPN}]_2[\text{H}_3\text{Rh}_{13}(\text{CO})_{24}]$ was prepared from $\text{Rh}_4(\text{CO})_{12}$ by the literature method.^{10a} The product was isolated in pure form as a dark brown solid after recrystallization from THF/isopropyl alcohol.

IR Measurements of Rhodium Cluster $\text{p}K_a$ Values. IR absorptivities in CH_3CN were determined as described in previous work.¹ The $\text{p}K_a$ values of $[\text{Rh}_{13}(\text{CO})_{24}\text{H}_3]^{2-}$ and $[\text{Rh}_{13}(\text{CO})_{24}\text{H}_2]^{3-}$ were determined by the methods used in previous work.^{1,17,18} When the $\text{p}K_a$ of $[\text{Rh}_{13}(\text{CO})_{24}\text{H}_3]^{2-}$ was being determined and only $[\text{Rh}_{13}(\text{CO})_{24}\text{H}_3]^{2-}$ and $[\text{Rh}_{13}(\text{CO})_{24}\text{H}_2]^{3-}$ were present, overdetermined least-squares methods were used to determine the best value of x (the mole fraction of T which was $\text{H}_3\text{Rh}_{13}^{2-}$) from the known total concentration T and A_{2019} and A_{1992} (eqs 4 and 5). When the $\text{p}K_a$ of $[\text{Rh}_{13}(\text{CO})_{24}\text{H}_2]^{3-}$ was being determined, the equilibrium concentration of $\text{H}_2\text{Rh}_{13}^{3-}$ was calculated from $\epsilon_{(\text{H}_2\text{Rh}_{13}^{3-} \text{ at } 1992)}$ and A_{1992} , and the equilibrium concentration of $\text{H}_1\text{Rh}_{13}^{4-}$ was obtained by subtracting $[\text{H}_2\text{Rh}_{13}^{3-}]$ from the total concentration of $\text{H}_2\text{Rh}_{13}^{3-}$ initially present.

Kinetics of Deprotonation of Rhodium Clusters. All kinetic measurements were carried out with a Masterline Model 2095 constant temperature bath. Temperatures were held constant to within 0.1 °C. An acetonitrile solution of the hydride was prepared at known concentration on the high-vacuum line. An appropriate amount of base solution was added by syringe in the inert-atmosphere glovebox. Total base concentrations were varied over a range from 0.05 to 0.5 M depending on the base used and the rate of reaction. After base was added, the solution was frozen at -196 °C until the start of the experiment. The reaction was followed by IR spectroscopy (the terminal CO stretch of $[\text{H}_3\text{Rh}_{13}(\text{CO})_{24}]^{2-}$ at 2019 cm^{-1}).

When each aliquot was taken, the reaction was first fast-quenched by a brief dip in liquid nitrogen and then placed in an ice bath during sampling. The aliquot was drawn from the solution with a nitrogen-purged syringe and injected into the nitrogen-purged CaF_2 cell, which was immediately placed in the spectrophotometer and scanned. The solution was then returned to the constant-temperature bath.

At least three data points were recorded per half-life, and the reactions were followed for at least 3 half-lives. Infinity points employed in the calculation of pseudo-first-order rate constants were measured after 10 half-lives.

The forward rate constant k_{H^+} in the $[\text{Rh}_{13}(\text{CO})_{24}\text{H}_3]^{2-}/p\text{-CF}_3\text{C}_6\text{H}_4\text{NH}_2$ system (eq 9) was obtained by fitting y (the molar extent of reaction) as a function of time to the approach-to-equilibrium eq 15,³⁰ where a is the initial concentration of $[\text{Rh}_{13}(\text{CO})_{24}\text{H}_3]^{2-}$, b is the known total concentration of $p\text{-CF}_3\text{C}_6\text{H}_4\text{NH}_2$, and y_e is the observed value of y at equilibrium. At each aliquot time t values of y were calculated by overdetermined least-squares methods from the known total concentration of $[\text{Rh}_{13}(\text{CO})_{24}\text{H}_3]^{2-}$ and $[\text{Rh}_{13}(\text{CO})_{24}\text{H}_2]^{3-}$ and from the observed values of A_{2019} and A_{1992} (eqs 4 and 5).

$$\ln \left[\frac{y[ab - (a+b)y_e + aby_e]}{ab(y_e - y)} \right] = k_{\text{H}^+} \frac{2ab - (a+b)y_e}{y_e} t \quad (15)$$

Acknowledgment. This research was supported by NSF Grant CHE-8819760. We thank S. Soley Kristjansdóttir for assistance with the approach-to-equilibrium calculations and Bruce Bender for the translation of ref 10c.

(27) (a) Chini, P. *J. Chem. Soc., Chem. Commun.* **1967**, 29. (b) Chini, P.; Albano, V. *J. Organomet. Chem.* **1968**, 15, 433.

(28) McCleverty, J. A.; Wilkinson, G. *Inorg. Synth.* **1966**, 8, 211.

(29) Cattermole, P. E.; Osborne, A. G. *Inorg. Synth.* **1977**, 17, 115.

(30) Moore, J. W.; Pearson, R. G. *Kinetics and Mechanism. A Study of Homogeneous Chemical Reactions*, 3rd ed.; Wiley: New York, 1981; p 306.